

Journal of Materials Chemistry A

Accepted Manuscript



This is an *Accepted Manuscript*, which has been through the Royal Society of Chemistry peer review process and has been accepted for publication.

Accepted Manuscripts are published online shortly after acceptance, before technical editing, formatting and proof reading. Using this free service, authors can make their results available to the community, in citable form, before we publish the edited article. We will replace this *Accepted Manuscript* with the edited and formatted *Advance Article* as soon as it is available.

You can find more information about *Accepted Manuscripts* in the [Information for Authors](#).

Please note that technical editing may introduce minor changes to the text and/or graphics, which may alter content. The journal's standard [Terms & Conditions](#) and the [Ethical guidelines](#) still apply. In no event shall the Royal Society of Chemistry be held responsible for any errors or omissions in this *Accepted Manuscript* or any consequences arising from the use of any information it contains.

ARTICLE

Ultra-thin SiC Layers Covered Graphene Nanosheets as Advanced Photocatalysts for Hydrogen Evolution

Cite this: DOI: 10.1039/x0xx00000x

Xunfu Zhou^a, Qiongzhi Gao^a, Xin Li^{a,*}, Yingju Liu^a, Shengsen Zhang^a, Yueping Fang^{a,*}, Jun Li^{b,*}Received 00th January 2012,
Accepted 00th January 2012

DOI: 10.1039/x0xx00000x

www.rsc.org/

Herein, for the first time, the ultra-thin SiC nanoparticles or ultra-thin layers covered graphene nanosheets were successfully prepared via using a facile in-situ vapor-solid reaction. The samples were characterized by X-ray diffraction, UV-visible spectroscopy, photoluminescence spectra analysis, Raman spectra, transient photocurrent responses and transmission electron microscopy. The photocatalytic activities were also evaluated by H₂ evolution from pure water or water containing Na₂S as an electron donor. The resulting SiC-graphene hybrids show enhanced photocatalytic H₂-evolution activities in the presence of an electron donor. Especially, the graphene nanosheet and SiC nanocrystal hybrids show the highest photocatalytic activity in H₂ production under visible light, which is about 10 times higher than that of the SiC nanocrystals. The enhanced activities of the SiC-graphene hybrids can be attributed to their 2D nanosheet structures, large surface area, enhanced visible-light absorption and rapid interfacial charge transfer from SiC to graphene. Our results can provide an effective approach to synthesize graphene-based heterogeneous nanocomposites for a wide variety of potential applications in solar energy conversion and storage, separation, and purification processes.

1. Introduction

Hydrogen has been considered as one of the most promising alternatives for classical fuels due to its high energy capacity and environmentally friendly combustion product (water).^{1,2} If hydrogen is generated by energy from a sustainable source such as solar energy, it can then serve as a green energy carrier in the future society. Thus, since Honda and Fujishima discovered photocatalytic H₂ evolution over TiO₂ in 1972,³ photocatalytic hydrogen generation from water splitting using solar energy and semiconductors has drawn a lot of attention and has been regarded as one of the most important approaches to solving the problems of global energy crisis and environmental pollution. In general, the activity of a given semiconductor for water splitting is strongly determined by several key factors, such as light harvesting, charge separation and transportation, surface catalytic efficiency (charge utilization) and photostability.⁴ Among them, the interfacial charge-transfer processes plays a decisive role in enhancing its activity for water splitting.⁵ In the past 40 years, many exciting breakthroughs have been made.⁶ A large number of metal oxide semiconductor photocatalysts with d⁰ or d¹⁰ electronic configurations, such as TiO₂, Ta₂O₅, WO₃ and Ga₂O₃, have been reported.⁷ More importantly, to efficiently utilize the visible light accounting for 43% of the solar energy, various kinds of visible-light-driven photocatalysts have continuously emerged in recent years,⁸⁻¹⁰ such as CdS,⁸ SiC,⁹ carbon nanotubes/SiC nanowires,¹⁰

C₃N₄,¹¹ Cu₂O¹² and so on. However, none of them could satisfy all the requirements such as low toxicity and cost, high stability, and excellent visible-light activity for various practical applications. Thus, it is still a great challenge to develop highly stable and efficient visible-light-driven photocatalysts through exploiting new narrow-band semiconductors or engineering the existing ones.^{4,6}

Silicon carbide (SiC) is an important semiconductor material with proper band gap (2.4 eV for 3C-SiC and 3.3 eV for 2H-SiC at room temperature) for visible-light absorption.¹³ Furthermore, it is stable, nontoxic and abundant. In particular, 3C-SiC has a suitable conduction band potential (E_{CB} for SiC = -0.9 V vs NHE at pH 7) for water splitting. However, there are one inherent drawbacks for SiC: fast recombination rate of photo-generated electron-hole pairs.^{14, 15} To improve photocatalytic activity of SiC photocatalysts, nanostructured SiC (e.g. quantum dots,¹⁶ nanoparticles,¹⁷ nanowires,¹⁸ hollow spheres¹⁹) and SiC-based heterojunction photocatalysts (e.g. SiC/TiO₂,²⁰ SiC/MoS₂,²¹ SiC/SnO₂ and SiC/CdS,^{19,22} as well as SiC/graphene hybrids^{18, 23, 24}) have been also widely explored. Although these SiC/graphene hybrids reported previously exhibit improved activities for water splitting, the large size of the SiC particles and the loose contact between SiC particles and graphene in these hybrids were not ideal for achieving efficient electron transfer across the interfaces, thus greatly limiting the degree of activity enhancement. One of the most promising strategies is to establish the intimate interfacial

contact between graphene and semiconductor to efficiently boost the catalytic performances of graphene-based photocatalysts. It is generally accepted that the high activity of graphene-semiconductor hybrids is attributed to the role of graphene as a highly conductive scaffolds to facilitate electron trapping and transport.²⁵⁻²⁸ Thus, optimizing the Schottky-type heterojunctions between graphene and semiconductor through improving their interfacial properties is a critical approach to rationally design highly efficient graphene-semiconductor photocatalysts. For example, a highly recyclable photocatalytic activity for methyl orange pollutant was achieved by in situ growth of ultradispersed mesoporous TiO₂ nanocrystals on graphene aerogels through the formation of Ti–O–C and Ti–C bonds which were favorable to charge transfer.²⁹ To the best of our knowledge, there has been no report on the *in-situ* formation of ultra-thin carbide semiconductor nanocrystals on graphene nanosheets using graphene as carbon source and the application of such materials in photocatalytic water splitting.

In the present work, we attempted to develop a general method for in-situ growth of ultrafine SiC nanocrystals (NCs) on the surface of graphene sheets (GSs). Through controlling the reaction time, two types of SiC-graphene hybrids with increasing SiC contents were obtained, including (1) small amount of SiC as nanocrystals (nanoparticles or ultrathin layers) attached on GSs-denoted as GSs/SiC; and (2) larger amount of SiC as thin films encapsulating GSs - denoted as GSs@SiC, respectively. Due to the nanosheet structures and the formation of tight Schottky-type junctions between SiC and graphene, the GSs/SiC and GSs@SiC exhibit more pronounced enhancements in H₂ production over the SiC NCs. Especially, the GSs/SiC shows the highest photocatalytic activity in H₂ production under visible light, which is about 10 times higher than that of the comparable SiC NCs.

2. Experimental Section

Chemicals and materials

All chemicals were of analytical grade and used as received without further purification. Nitric acid, hydrofluoric acid and sodium sulphide were purchased from Sino pharm Chemical Reagent Co., Ltd. Graphene sheets (GSs, specific surface area of more than 90 m².g⁻¹) were purchased from Nanjing XFNANO Materials Tech Co., Ltd. (See Supporting Information). Micro-grade silicon powder (99.99% metals basis, 40-200 mesh) was supplied by Aladdin Reagents (Shanghai) Co., Ltd.

Preparation of SiC-GS hybrids

The GSs as precursor were uniformly mixed with excess micro-grade silicon powder, and the prepared mixture was placed in the center of the tube furnace. It was then heated to 1320 °C at a heating rate of ~ 3 °C min⁻¹ in an argon atmosphere and maintained at this temperature for variable time. The argon used in this study is 99.99% argon with oxygen of 10 ppm. Afterwards, the resulting products were treated with 1:3 HF-HNO₃ aqueous solutions for 12 h to remove the excess silicon, finally dried at 100 °C.

Preparation of SiC NCs for comparison

The SiC NCs were prepared through heating the GSs and silicon powder in an argon atmosphere at 1320°C for 1h and keeping the

other parameters constant for the SiC/GS hybrids (See Supporting Information for details).

Material Characterization

The surface morphologies of the as-prepared samples were observed by thermal field emission environment scanning electron microscopy (FE-SEM, FEI, Quanta 400), and transmission electron microscopy (TEM, JEM-2010HR). The compositions and structures of the products were analyzed by X-ray diffraction (XRD, D8 ADVANCE X-ray diffractometer, Cu K α radiation $\lambda=0.15418$ nm) with a scanning rate of 10° min⁻¹ in the 2-theta range from 2° to 80° and laser Raman spectroscopy (Renishaw in Via). Thermogravimetric (TG) analyses were carried out on a Netzsch TG 209 apparatus under a flow rate of 50 ml min⁻¹ air. A Shimadzu spectrophotometer (model 2501 PC) equipped with an integrating sphere was used to record the UV-vis diffuse reflectance spectra of the samples. The excitation and emission spectra were recorded with an F-4500 spectrophotometer equipped with a 150 W Xenon lamp as the excitation source.

Photocurrent measurements were carried out in a Zennium electrochemical workstation (ZAHNER) coupled with a Xe lamp (PLS-SXE300UV, TrustTech, China) using a standard three-compartment cell and applying a bias of 0.1 V. The wavelengths of the incident light were greater than 400 nm through a UV-400 filter. ITO/SiC/GSs, ITO/SiC@GSs or ITO/bulk SiC crystals were acted as working electrode. A Pt wire and Ag/AgCl electrode were used as the counter electrode and the reference electrode, respectively. 0.1 M KCl aqueous solution and 0.5 M Na₂SO₄ solution were employed as electrolytes, respectively.

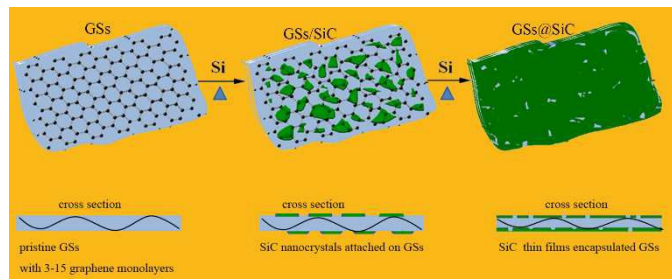
Photocatalytic water splitting

Photocatalytic water splitting was carried out in a LabSolar H₂ photocatalytic hydrogen evolution system (Perfectlight, Beijing). A 300W Xe arc lamp (PLS-SXE300, Beijing Trusttech) with a UV-cutoff filter (providing visible light $\lambda \geq 420$ nm) was used as a visible light source and was positioned 1 cm away from the reactor. The average light intensity of 160 mW.cm⁻² was measured with a Si photodiode (FZ-A, HANDY). In a typical reaction, 50 mg of the sample powder, such as GSs/SiC, GSs@SiC and SiC NCs, was dispersed in a Pyrex glass reactor containing 100 mL of Na₂S (0.1 M) solution or distilled water. Then the system was sealed and vacuumized to keep the pressure as -0.09 MPa. Afterwards, a circular cooling water system was turned on and the reactor was irradiated with Xe lamp (300 W) under magnetic stirring. The gases evolved were analyzed on line with gas chromatography (GC-7900, TCD, with N₂ as carrier gas) after 1 h of illumination. The reaction was continued for 5 h. The experiment was repeated to investigate the photocatalytic stability of the SiC-GS hybrids. After 5 h of the reaction, H₂ produced was evacuated, and then for another 5 h run.

3. Results and Discussion

The fabrication of SiC-GS hybrids is schematically illustrated in Scheme 1. The pristine GSs have the thickness of 1-5 nm and the specific surface area of 90 m² g⁻¹, which should consist of a stack of 3-15 graphene monolayers (See Supporting Information). Because the silicon melting points and

sublimation temperature is 1420 °C and 1127 °C, respectively, we resorted to a vapor-solid reaction [see Eq. (1)] for preparing SiC-GS hybrid samples. During this process, the GSs and silicon powders were mixed and heated to 1320 °C in an argon atmosphere. After the vapor-solid reaction between the GSs and Si powders for 10 min and 20 min, it produced two types of samples labeled as GSs/SiC and GSs@SiC, respectively.



Scheme 1. Fabrication of SiC-GS hybrids.

The morphology and microstructure of the as-prepared samples were initially investigated by scanning electron microscopy (SEM) and transmission electron microscopy (TEM). As shown in Figure 1, after the vapor-solid reaction at 1320 °C between solid GSs and Si vapor, the GSs is no longer soft and clean. Instead, they present a curled sheet-like structure with rough surfaces (A-D) in comparison to the smoother pristine GSs (See Supporting Information for details). It can be seen that a lot of small nanoparticles or thin layers was grown on the surface of the curled nanosheets (A and B) in the initial period, which was then converted into slightly thicker continuous films in longer reaction time (C and D).

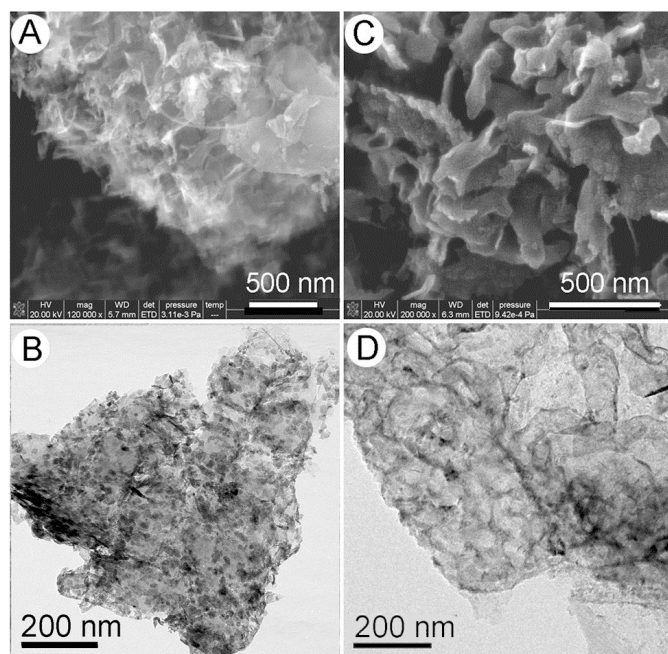


Figure 1. SEM and TEM images of the two types of samples: (A, B) GSs/SiC; (C, D) GSs@SiC.

The nature of above morphological changes of the as-prepared samples was further investigated using XRD and

Raman analysis. Figure 2 shows XRD patterns and Raman spectra of the as-prepared two samples. The XRD pattern in Figure 2A provides clear evidence that the GSs/SiC and the GSs@SiC are composed of two mixed solid phases, namely SiC (JCPDS card No 29-1129)^{18, 30} and GSs, indicating that SiC nanoparticles (and/or thin flakes) and films have the high crystallinity and grown on the surface GSs after the vapor-solid reaction for 10 min and 20 min, respectively.

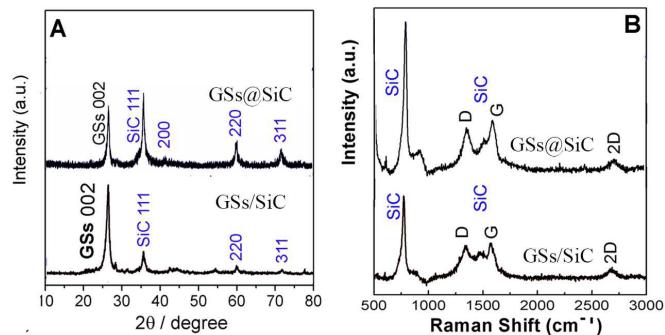


Figure 2. Typical XRD patterns (A) and Raman spectra (B) of the GSs/SiC and GSs@SiC.

The observed SiC nanoparticles and thin layers or films are further confirmed by Raman scattering measurements shown in Figure 2B. Raman fingerprint peaks of SiC are identified at 772 and 1506 cm^{-1} in all three samples.³¹ Raman fingerprint peaks of graphene, including D, G and 2D bands, are well identified at 1347, 1578, and 2680 cm^{-1} on the curve of GSs/SiC and GSs@SiC.

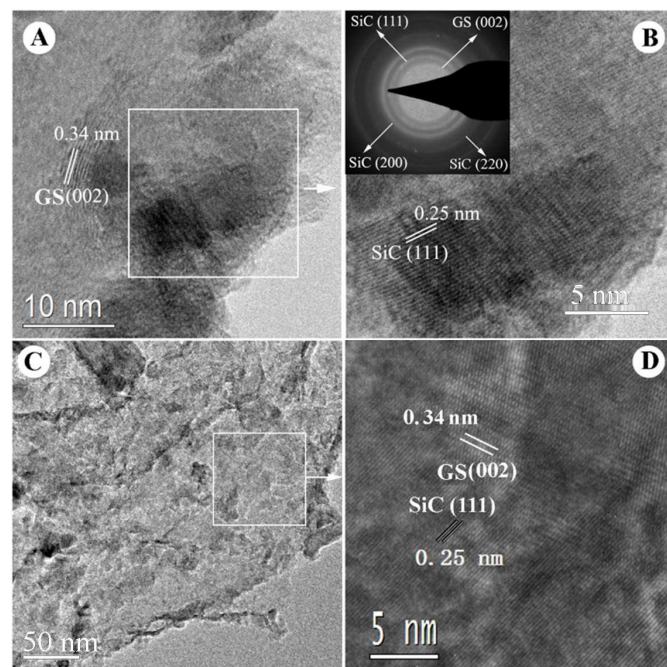


Figure 3. TEM, HRTEM images of the GSs/SiC (A and B), GSs@SiC (C and D); Inset in B is the corresponding ED pattern of the GSs/SiC; B and D are taken from the white squares in A and C, respectively.

The total SiC content of the two samples was determined by TGA. The mass fraction of the SiC in the two samples can be

easily estimated to be about 22.92 wt. % for the GSs/SiC and 44.94 wt. % for the GSs@SiC, respectively (See Supporting Information for details, Fig. S3). In addition, characterized by nitrogen adsorption and desorption isotherms, the specific surface areas of the GSs/SiC and GSs@SiC are found to be 72 and 57 m² g⁻¹, respectively.

The perfect heterojunction with the superior intrinsic contact in GSs/SiC and GSs@SiC were further examined with TEM, HRTEM images and electron diffraction patterns, as shown in Figure 3. One can immediately see the rough surface characteristics of the GSs/SiC (A) and GSs@SiC (C). Three HRTEM images (A, B and D) show clear lattice fringes for the (002) planes of GSs, with the d spacing of 0.34 nm, and the (111) planes of SiC, with the d spacing of 0.25 nm. The electron diffraction patterns (inset in Figure 3A) can be indexed to SiC and the GSs, respectively. Obviously, the (002) planes of GSs and the (111) planes of SiC are integrated together to form the perfect heterojunction with the superior intrinsic contact. Furthermore, three HRTEM images (A, B and D) indicate also that the SiC coating have the high crystallinity. To the best of our knowledge, this is the first evidence of the application of graphene as both carbon sources and 2D templates in constructing ultra-thin layered metal-free semiconductor heterojunction. Further studies on the extension of the synthetic strategy to *in-situ* prepare the composite photocatalysts with 2D layered heterojunctions through coupling graphene and other carbon-containing semiconductors are currently underway.

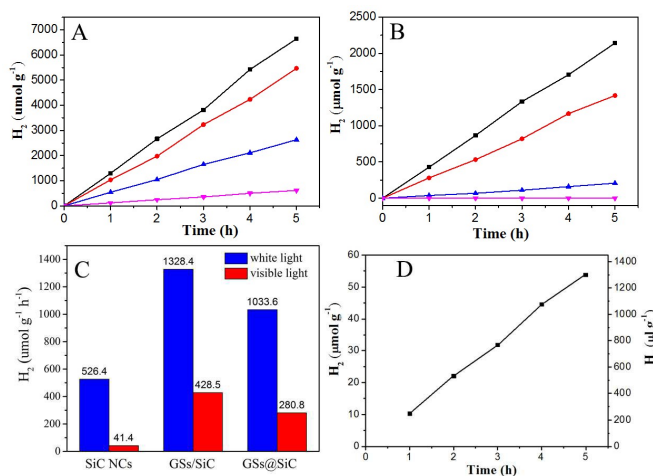


Figure 4. The total amount of H₂ produced under the photocatalysis of four samples: (a) GSs/SiC, (b) GSs@SiC, (c) SiC NCs and (d) GSs for comparison under white light illumination (A) and visible light irradiation (B), respectively; (C) their corresponding average hydrogen production rates; (D) The total amount of H₂ produced of the GSs/SiC in distilled water without any sacrificial reagent under visible light.

We investigated the potential use of the novel SiC-GS hybrids as photocatalysts for splitting water under white light illumination (a 300 W xenon lamp) and visible light irradiation (a 300 W xenon lamp, λ ≥ 420 nm). The results of photocatalytic hydrogen production over the three samples from a Na₂S solution under white light illumination and visible light irradiation are shown in Figure 4. It can be seen that the total amount (A and B) of H₂ evolved increases nearly linearly

with the irradiation time over a 5-hr period for all samples. The total H₂-production amounts in 5 h over GSs/SiC, GSs@SiC and the SiC NCs (A) under white light illumination were 6642, 5168 and 2632 μmol g⁻¹, respectively. The total amount of hydrogen production for the GSs/SiC is about 2.5 times higher than that of the SiC NCs. However, under visible light irradiation, the GSs/SiC shows the most reactivity in H₂ production (B). The total H₂-production amounts in 5 h over GSs/SiC, GSs@SiC and the SiC NCs were 2142, 1418 and 207 μmol g⁻¹, respectively. Their corresponding H₂-production rate (C) is 1328.4/428.5, 1033.6/280.8 and 526.4/41.4 μmol g⁻¹ h⁻¹ under white light/visible light irradiation, respectively. It was very surprising that the GSs/SiC show the highest catalytic activity for H₂ production. The H₂ production rate of GSs/SiC is about 10 times higher than that of the SiC NCs under visible light irradiation.

In order to clarify the role of Na₂S, we investigated also the photocatalytic activity of the GSs/SiC for overall water splitting under visible irradiation in the absence of Na₂S. It can be seen that the total amount (D) of H₂ evolved increases nearly linearly with the irradiation time over a 5-hr period. The hydrogen production rate of the GSs/SiC is 54.8 μmol g⁻¹ h⁻¹ (1227.5 μl g⁻¹ h⁻¹), and higher than that of those SiC/graphene hybrids reported previously.^{18, 24} The results also confirmed that the H₂-production rate of the GSs/SiC from a Na₂S solution is much higher than that from a distilled water under visible light irradiation, due to the significantly suppressed recombination of photo-excited charge carriers.

Cyclic experiments were carried out to investigate the stability of the GSs/SiC. The H₂ evolution in different runs is also shown in Figure 5. No remarkable degradation of H₂ evolution is observed in the repeated runs for the photocatalytic reaction of 20 h under white light illumination and visible light irradiation, respectively.

To deeply understand the good stability and durability of the GSs/SiC, the structural morphology changes of the GSs/SiC after Cyclic experiments were studied. The TEM and HRTEM images, XRD patterns and UV-Vis spectra of the GSs/SiC after cyclic experiments are shown in Fig.S4 (See Supporting Information for details). As can be seen, no change in the morphology and nanostructure of the GSs/SiC after cyclic experiments occurred obviously. Only the XRD patterns show several characteristic peaks from impurities of SiO₂ because of oxidation of SiC surface.

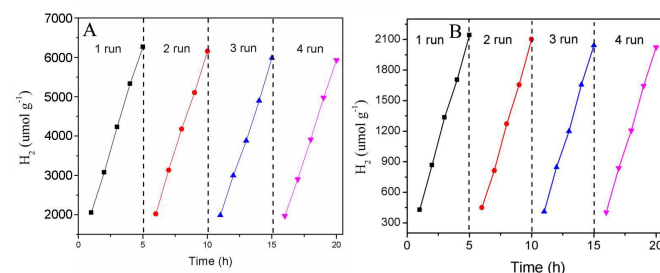


Figure 5. H₂ evolution of the GSs/SiC through four noncontinuous experiments: A) under white light; B) under visible light.

On basis of the above structure/morphology/activity investigations of our hybrids, we can attribute the enhanced performance of our SiC-GS hybrids over SiC NCs to their

nanosheet structures and interfacial charge transfer processes, created through hybridization of SiC with GSs, which can affect the performance in two different ways: (1) the GSs can act as photosensitizers through extending the absorption range and delivering additional electrons to the valence band (VB) of the SiC^{32,33} and (2) the GSs can act as electron acceptors for photoexcited electrons from the conduction band (CB) of the SiC, thus reducing electron-hole pair recombination and increasing the exciton lifetime.³⁴ Scheme 2 illustrates the electron-hole transfer mechanism in the GSs/SiC hybrids. In the absence of the graphene layers, most of these excited electrons recombine quickly with holes. Usually, only a small portion of electrons or holes participate in the photocatalytic reactions, resulting in low reactivity.

Interfacial charge transfer processes have been solely accounted for the modest enhancements in nanocarbon hybrids reported so far.³⁵ The more pronounced enhancements of the GSs/SiC and GSs@SiC over the SiC NCs may stem from the perfect heterojunction interface. Since the nature of the interface affects the efficiency of charge separation, the in-situ growth of the ultrafine SiC NCs or layers in the GSs/SiC and GSs@SiC forms a tight Schottky-type junction between the SiC and the GSs (Figure 3A, B and D), which is considered a metallic conductor due to the graphite-like interactions between the individual interfaces. Such a junction would enhance the charge separation through electron extraction by the GSs.³⁶

The photoluminescent (PL) decay and photocurrent spectra can be used as powerful tool for evaluation of charge transfer efficiency in the donor-acceptor blend composites.³⁴ Figure 6A shows the PL spectra of the samples. Under the 220 nm excitation, the SiC NCs shows a sharp PL peak at 480 nm. By contrast, a clear fluorescence drop in the GSs/SiC and GSs@SiC samples was seen, hence implying an increase in efficient charge separation between SiC layer and GSs in GSs/SiC and GSs@SiC. The PL drop is consistent with higher catalytic activity of GSs/SiC and GSs@SiC in H₂ production than that of the SiC NCs.¹⁵

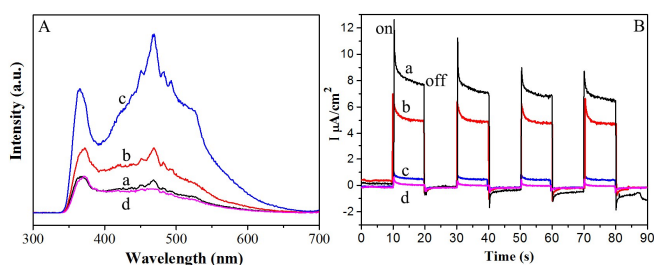


Figure 6. PL spectra (A) and transient photocurrent responses (B) of the SiC/GSs (a), GSs@SiC (b), SiC NCs (c) and (d) GSs for comparison.

The enhanced charge separation and solar energy utilization in photocatalysis could be further confirmed by the photoelectrochemical behaviour of composite materials. Their transient photocurrent responses under visible irradiation are shown in Figure 6B. Obviously, the photocurrent of SiC/GSs had dramatically increased after the hybridization of the SiC with GSs. The SiC/GSs had the largest photocurrent (about 8 $\mu\text{A}\cdot\text{cm}^{-2}$), which was about 16 times compared with that of the SiC NCs (about $0.5\mu\text{A}\cdot\text{cm}^{-2}$). Note that the photocurrent of the

SiC@GSs is $5\mu\text{A}/\text{cm}^2$. It is understandable that the higher photocurrent means that more photoinduced electrons can transfer from the as-collected product to the counter electrode at applied bias efficiently.²⁶

In addition, it can be seen from Figure 7 that the SiC NCs exhibits a wide absorption band from UV to visible light. For the SiC/GSs and GSs@SiC, a similar absorption band is present but the absorption band is stronger in the visible region. This indicates that the SiC/GSs and GSs@SiC have better response to the visible light.

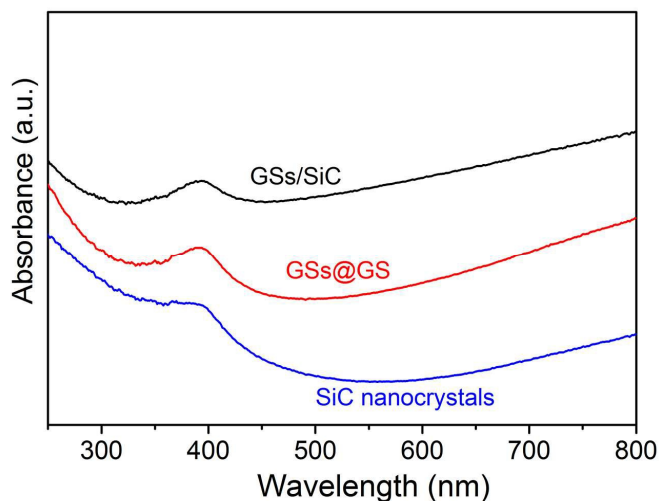
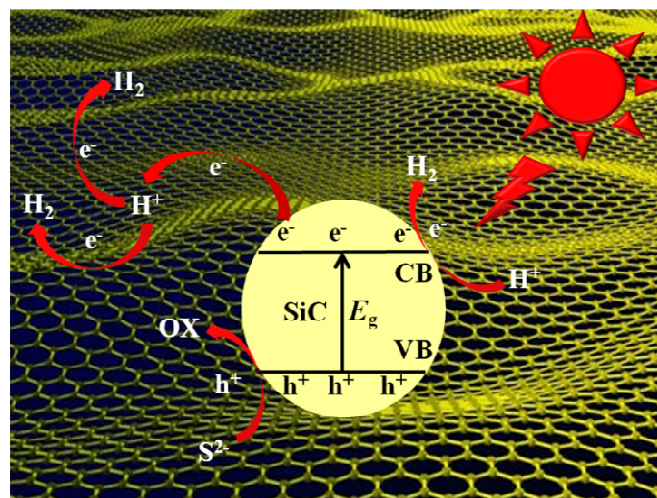


Figure 7. UV-Vis spectra of the SiC/GSs, GSs@SiC and SiC NCs.

In a word, the mechanism of photocatalytic process was shown in Scheme 2, the oxidation and reduction for sacrificial water splitting occurred on the surface of the SiC and GSs, respectively. For GSs/SiC, besides their perfect heterojunction interface, they have more exposed surface area of the GSs than that of other two samples, which directly contact with the reaction solution and benefits the adsorption and reduction of H⁺, thus favoring H₂ production. Therefore, the highest activity in H₂ production by GSs/SiC under visible light irradiation should be attributed to their large specific surface area and intimate interfacial contact, which could be achieved through loading the ultra-thin SiC nanoparticles or layers onto the exposed larger surface area of GSs.



Scheme 2. Schematic mechanism of photocatalytic process of the SiC-GS hybrids for H₂ evolution.

4. Conclusions

In summary, an in-situ growth method has been developed to prepare crystalline nanoparticles, ultra-thin layers or films of SiC on the GS surface by a vapor-solid reaction between GSs and Si powders. We also demonstrated that the photocatalytic properties of the produced SiC-GSs hybrids can be significantly improved by modifying the interfaces and morphology of the active SiC layer. The resulting hybrids exhibited very high activities and photostabilities in sacrificial photocatalytic water splitting. It is believed that the enhanced photocatalytic activity of the graphene-SiC hybrids is attributed to the synergistic effects between SiC nanocrystals and graphene nanosheets, including the high crystallinity of the SiC coating, large surface area, enhanced visible-light absorption, as well as the formation of an intimate Schottky-type junction between the GSs and the semiconducting SiC, which can enhance the ultrafast charge separation at the interface. Our results suggest that the SiC-GS hybrids, as promising nanocomposites, have great potential for the applications in photocatalysis, catalysis, solar-cell, separation, and purification processes.

Acknowledgements

This research was supported by NSF of China (21173088, 21475047 and 20906034). The authors thank the Foundation for High-level Talents in Higher Education of Guangdong Province and Guangdong Natural Science Foundation (2014A030310427). Special thanks to Prof. Can Li in State Key Laboratory of Catalysis, Dalian Institute of Chemical Physics, Chinese Academy of Sciences. This work also partly supported by the State Key Laboratory of Catalysis cooperation project (N-08-08) and the State Key Laboratory of Advanced Technology for Material Synthesis and Processing (2015-KF-7).

Notes and references

^a The institute of Biomaterial, College of Materials and Energy, South China Agricultural University, Guangzhou, Guangdong 510642, China. Fax: 8620-85285565; Tel: 8620-85285565; E-mail: ypfang@scau.edu.cn;

xinliscou@yahoo.com; junli@ksu.edu

^b Department of Chemistry, Kansas State University, Manhattan, KS 66506, United States.

† Electronic Supplementary Information (ESI) available: [SEM and TEM images, Raman spectrum, XRD pattern and TGA of the pristine GSs; TEM of the SiC NCs; TGA curves of the SiC/GSs and GSs@SiC; TEM and HRTEM images, XRD patterns and UV-Vis spectra of the SiC/GSs after four noncontinuous cyclic experiments]. See DOI: 10.1039/b000000x/

- 1 J.A. Turner, *Science*, 2004, **305**, 972-974.
- 2 L. Schlapbach, A. Züttel, *Nature*, 2001, **414**, 353-358.
- 3 A. Fujishima, K. Honda, *Nature*, 1972, **238**, 37-38.
- 4 Y. Qu, X. Duan, *Chem. Soc. Rev.*, 2013, **42**, 2568-2580.
- 5 P.V. Kamat, *J. Phys. Chem. Lett.*, 2012, **3**, 663-672.
- 6 X. Chen, S. Shen, L. Guo, S.S. Mao, *Chem. Rev.*, 2010, **110**, 6503-6570.
- 7 K. Maeda, K. Domen, *J. Phys. Chem. C*, 2007, **111**, 7851-7861.
- 8 Q. Wang, J. Li, Y. Bai, J. Lian, H. Huang, Z. Li, Z. Lei, W. Shangguan, *Green Chem.*, 2014, **16**, 2728-2735.

- 9 M. Wang, J. Chen, X. Liao, Z. Liu, J. Zhang, L. Gao, Y. Li, *Int. J. Hydrogen Energ.*, 2014, **39**, 14581-14587.
- 10 X.F. Zhou, X. Li, Q.Z. Gao, J.L. Yuan, J.Q. Wen, Y.P. Fang, W. Liu, S.S. Zhang, Y.J. Liu, *Catal. Sci. Technol.*, 2015, Advance Article, DOI: 10.1039/C4CY01757A.
- 11 X. Wang, K. Maeda, A. Thomas, K. Takanebe, G. Xin, J.M. Carlsson, K. Domen, M. Antonietti, *Nat. Mater.*, 2009, **8**, 76-80.
- 12 S. Zhang, S. Zhang, F. Peng, H. Zhang, H. Liu, H. Zhao, *Electrochem. Commun.*, 2011, **13**, 861-864.
- 13 M. Steenackers, I.D. Sharp, K. Larsson, N.A. Hutter, M. Stutzmann, R. Jordan, *Chem. Mater.*, 2009, **22**, 272-278.
- 14 Y. Nariki, Y. Inoue, K. Tanaka, *J. Mater. Sci.*, 25 (1990) 3101-3104.
- 15 W. Zhou, L. Yan, Y. Wang, Y. Zhang, *Appl. Phys. Lett.*, 2006, **89**, 013105.
- 16 C. He, X. Wu, J. Shen, P.K. Chu, *Nano Lett.*, 2012, **12**, 1545-1548.
- 17 J.Y. Hao, Y.Y. Wang, X.L. Tong, G.Q. Jin, X.Y. Guo, *Catal. Today*, 2013, **212**, 220-224.
- 18 Y.W. Wang, X.Y. Guo, L.L. Dong, G.Q. Jin, Y.Y. Wang, X.Y. Guo, *Int. J. Hydrogen Energ.*, 2013, **38**, 12733-12738.
- 19 X. Zhou, Y. Liu, X. Li, Q. Gao, X. Liu, Y. Fang, *Chem. Commun.*, 2014, **50**, 1070-1073.
- 20 J. Akikusa, S.U.M. Khan, *Int. J. Hydrogen Energ.*, 2002, **27**, 863-870.
- 21 X. Guo, X. Tong, Y. Wang, C. Chen, G. Jin, X.-Y. Guo, *J. Mater. Chem. A*, 2013, **1**, 4657-4661.
- 22 Y. Peng, Z. Guo, J. Yang, D. Wang, W. Yuan, *J. Mater. Chem. A*, 2014, **2**, 6296-6300.
- 23 K.X. Zhu, L.W. Guo, J.J. Lin, W.C. Hao, J. Shang, Y.P. Jia, L.L. Chen, S.F. Jin, W.J. Wang, X.L. Chen, *Appl. Phys. Lett.*, 2012, **100**, 4.
- 24 J.J. Yang, X.P. Zeng, L.J. Chen, W.X. Yuan, *Appl. Phys. Lett.*, 2013, **102**, 4.
- 25 Y. Zhang, N. Zhang, Z.R. Tang, Y.J. Xu, *Phys. Chem. Chem. Phys.*, 2012, **14**, 9167-9175.
- 26 Q. Xiang, J. Yu and M. Jaroniec, *J. Am. Chem. Soc.*, 2012, **134**, 6575-6578.
- 27 T. Jia, A. Kolpin, C. Ma, R. C.-T. Chan, W.-M. Kwok and S. E. Tsang, *Chem. Commun.*, 2014, **50**, 1185-1188.
- 28 Q. Xiang and J. Yu, *J. Phys. Chem. Lett.*, 2013, **4**, 753-759.
- 29 B. Qiu, M. Xing, J. Zhang, *J. Am. Chem. Soc.*, 2014, **136**, 5852-5855.
- 30 J.Y. Hao, Y.Y. Wang, X.L. Tong, G.Q. Jin, X.-Y. Guo, *Int. J. Hydrogen Energ.*, 2012, **37**, 15038-15044.
- 31 J.Q. Hu, Q.Y. Lu, K.B. Tang, B. Deng, R.R. Jiang, Y.T. Qian, W.C. Yu, G.E. Zhou, X.M. Liu, J.X. Wu, *J. Phys. Chem. B*, 2000, **104**, 5251-5254.
- 32 C. Chen, W. Cai, M. Long, B. Zhou, Y. Wu, D. Wu, Y. Feng, *Acc Nano*, 2010, **4**, 6425-6432.
- 33 Y. Zhang, N. Zhang, Z.R. Tang, Y.J. Xu, *Acc Nano*, 2012, **6**, 9777-9789.
- 34 I.V. Lightcap, T.H. Kosel, P.V. Kamat, *Nano Lett.*, 2010, **10**, 577-583.
- 35 D. Eder, *Chem. Rev.*, 110 (2010) 1348-1385.
- 36 D. Sinha, J.U. Lee, *Nano Lett.*, 2014, **14**, 4660-4664.
- 37 T. Maassen, J.J. van den Berg, N. Ijbema, F. Fromm, T. Seyller, R. Yakimova, B.J. van Wees, *Nano Lett.*, 2012, **12**, 1498-1502.

Graphical abstracts

An in-situ growth method has been developed to prepare SiC-graphene hybrids, which exhibit high activities and photostabilities for water splitting.

